

Morphological wetting transitions at chemically structured surfaces

Reinhard Lipowsky*

MPI für Kolloid- und Grenzflächenforschung, Am Mühlberg, D-14476 Golm, Germany

Abstract

Chemically structured surfaces are discussed which consist of patterns of lyophilic and lyophobic surface domains. Wetting layers on top of these surfaces attain a variety of morphologies and undergo morphological wetting transitions. One convenient way to explore these transitions experimentally is by changing the total volume of the wetting layer. © 2001 Elsevier Science Ltd. All rights reserved.

Keywords: Wetting; Dewetting; Contact angle; Line tension; Structured surface

1. Introduction

A liquid droplet placed on top of an unstructured surface with a flat topography and a laterally uniform composition is characterized by a well-defined contact angle. If the liquid wets the surface, this contact angle is small and may even vanish, corresponding to partial and complete wetting, respectively. It was realized approximately two decades ago, that one may have a transition from partial to complete wetting [1,2] as one varies a certain control parameter such as the composition of the liquid [3].

Now, consider a chemically structured surface consisting of lyophilic and lyophobic surface domains as schematically shown in Fig. 1. The lyophilic and lyophobic domains are characterized by small and large contact angle, respectively. It was recently shown [4••,5••] that such a surface leads to morphological wetting transitions at which the shape of the wetting layer changes in a characteristic and typically abrupt manner.

2. A wide range of surface domain sizes

During the last decade, experimentalists have developed many methods by which one can prepare chemically structured surfaces with surface patterns as shown in Fig. 1. Here and below, the lyophilic and lyophobic domains are denoted by γ and δ , respectively. The basic length scale of these surface domain patterns is provided by the linear size L_γ of the lyophilic γ domains which can vary from the millimeter regime all the way down to the nanometer regime.

In the millimeter range, one may use screen printing technology in order to print hydrophobic coatings on glass surfaces [6•] or printed circuit board technology in order to create lyophilic domains for molten tin-lead alloys as applied in soldering processes [7•].

Several methods have been used to create structured surfaces with surface domains in the micrometer range: (i) elastomer stamps by which one can create patterns of hydrophobic alkanethiol on metal surfaces [8–11•]; (ii) vapor deposition through grids which cover part of the surface [12]; (iii) photolithography of amphiphilic monolayers which contain photosensitive molecular groups [13••]; (iv) domain formation in Langmuir–Blodgett monolayers transferred

*Tel.: +49-331-567-9600; fax: +49-331-567-9602.

E-mail address: lipowsky@mpig-golm.mpg.de (R. Lipowsky).

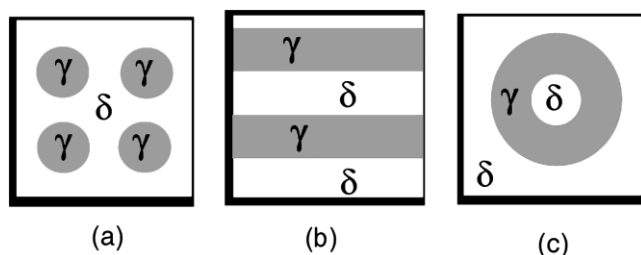


Fig. 1. Top view of structured surfaces which contain lyophilic γ domains (gray) within a lyophobic matrix δ (white). (a) A regular pattern of circular γ domains; (b) a pattern consisting of γ stripes; and (c) a ring-shaped γ domain. The width of the γ domains is denoted by L_γ .

to solid substrates [14•]; (v) unstable monolayers produced by such monolayer transfer [15••]; (v) electrophoretic assembly of colloids [16•]; or (v) anisotropic rupture of polymer films on top of a polymeric surface [17•].

Furthermore, new experimental methods are being developed in order to construct patterns with even smaller domain sizes in the nanometer range. These methods include lithography with colloid monolayers [18], atomic beams modulated by light masks [19], microphase separation in diblock copolymer films [20], or local oxidation of silicon surfaces induced by atomic force microscopy [21•].

3. Wetting of structured surfaces

Now, consider such a surface with a pattern of surface domains in contact with the bulk phase α , and let us place a certain amount of β phase on top of this surface. In general, the α and the β phase may represent any type of material and, thus, can be fluid or solid. In order to be specific, we will focus on the situation in which the β phase is a liquid and the α phase is a vapor or another liquid.

After the β phase has been deposited on the structured surface, it will form a wetting layer which tries to maximize its contact area with the lyophilic γ domains, and, at the same time, tries to minimize the total area of the $\alpha\beta$ interface. Depending on the shape and the pattern of these surface domains, the β phase may form a variety of different wetting morphologies and may undergo transitions between these morphologies. One convenient control parameter by which one can explore these transitions experimentally is the total volume V_β of the wetting layer. From a theoretical point of view, this corresponds to the canonical ensemble.

3.1. Volume as control parameter

The volume V_β of the β phase can be varied systematically in several types of experiments:

1. The β phase is a non-volatile liquid and the exchange of molecules between the α and the β phase can be ignored on the relevant time scales. In this case, the volume of the β phase is fixed and does not change during the wetting process. If one droplet of β phase is placed on a *single* lyophilic γ domain, it will try to spread over the whole domain. The final state will usually correspond to a state of minimal free energy. The situation is somewhat more complex if the initial β drop is large and covers *several disconnected* γ domains. In such a situation, the state of minimal free energy may correspond to an ensemble of several β droplets, but the β phase may not be able to attain this state since it involves a change in its topology. In other words, the rupture of the initial β drop into several β droplets may represent a relatively large activation barrier which prevents the β phase from attaining its state of minimal free energy. In such a situation, the wetting layer morphology represents a state which is only locally stable or metastable.
2. The β phase is a volatile liquid which condenses from a supersaturated vapor or liquid mixture α onto the γ domains. Indeed, the activation barriers for surface nucleation at the γ domains vanish for small contact angle $\theta = \theta_\gamma$ and, thus, can be much smaller than the activation barriers for homogeneous nucleation in the bulk α phase. The β phase will then start to condense on the γ domains even though the bulk α phase does not decay and remains in its metastable state. In this case, the total amount of β phase increases with time, but if this growth process is slow, the resulting time evolution of the droplet morphology will correspond to a sequence of equilibrium states with a certain volume of condensed β phase.
3. The β phase is a volatile liquid in thermal and chemical equilibrium with the α phase. In this case, the total amount of β phase is determined by the total volume of the system, by the total number of particles, and by the particle number densities of the α and β phases according to the usual lever rules.

3.2. Reference volume defined by surface domains

It turns out that any pattern of lyophilic γ domains can be characterized by a certain reference volume V_γ which is defined as follows. First, let us focus on the position of the $\gamma\delta$ domain boundaries between the lyophilic γ and the lyophobic δ domains. For the three patterns displayed in Fig. 1a–c, these domain

boundaries are circles, parallel lines, and concentric circles, respectively. These boundaries may be diffuse on the molecular scale, and one then has to use an appropriate convention in order to define the position of these domain boundaries in terms of the composition profile along the structured surface.

The shape of any wetting layer placed on this structured surface is characterized by constant mean curvature M as follows from the well-known Laplace equation. Now, consider all wetting layers for which the contact line is pinned to the $\gamma\delta$ domain boundaries. The shapes of these different wetting layers will, in general, be characterized by different mean curvatures. However, differential geometry provides some general theorems [22–26] which imply that, for any prescribed position of the contact line, there exists a shape of *maximal* mean curvature $M = M_{\max}$. Therefore, if one considers the situation in which the contact line is pinned to the $\gamma\delta$ domain boundaries, any pattern of surface domains can be characterized by a unique constant mean curvature shape with $M = M_{\max}$. The volume of this latter shape provides a *unique reference volume* $V = V_\gamma$.

It is instructive to discuss some examples. Thus, let us again consider the surface patterns shown in Fig. 1. For the circular γ domains shown in Fig. 1a, the maximal mean curvature shapes consist of *half spheres* which have the same diameter L_γ as the circular domains. Thus, the reference volume V_γ is equal to $V_\gamma = N(\pi/12)L_\gamma^3$ where N denotes the number of domains. For the long γ stripes shown in Fig. 1b, the maximal mean curvature shapes are *half cylinders* the diameter of which is equal to the width L_γ of the stripes. Finally, for the annulus domain in Fig. 1c, the maximal mean curvature shape is a nodoid as calculated in [7•].

3.3. Small volume limit

Next, consider the situation in which the volume V_β is very small compared to the reference volume V_γ . The β phase will then start to form a submonolayer, a monolayer or a few layers on the γ domains. The thickness of this ultrathin layer is determined by the force potentials between the molecules in the β phase and the structured substrate. After this thin film has been formed, additional deposition of β phase will lead to small droplets on the γ domains with contact angle $\theta = \theta_\gamma$. These droplets will grow until their contact lines reach the $\gamma\delta$ domain boundaries and the wetting layer covers all lyophilic γ domains completely.

Thus, in the regime with $V_\beta \ll V_\gamma$, each γ domain can accommodate a certain amount of β phase with a contact angle θ which is of the order of $\theta = \theta_\gamma$ (if the $\gamma\delta$ domain boundary is not circular, the contact angle

θ is not constant along this domain boundary). In this way, the β phase can maximize its contact with the γ domains without a disproportionate increase in the area of the $\alpha\beta$ interface. Thus, for small V_β , the β phase will form small ‘pancakes’ on all γ domains.

3.4. Large volume limit

Now, consider the opposite limit of large $V_\beta \gg V_\gamma$. Since the total area of the $\alpha\beta$ interface must grow at least as $\sim V_\beta^{2/3}$ for large V_β , the β phase will now prefer to form one large drop in order to minimize this interfacial area. If the lyophobic part of the structured surface is only weakly lyophobic, i.e. if the contact angle θ_δ is not too large, the drop will typically cover many surface domains and its contact line will move across both γ and δ domains.

In such a situation, the contact line will exhibit undulations with a wavelength which is comparable to the size L_γ of the surface domains. These undulations lead to folds in the $\alpha\beta$ interface which emanate from the contact line and have a linear extension of the order of L_γ [27•]. On length scales which are large compared with L_γ , one may then define an effective contact angle θ_{eff} via the Cassie equation [27•,28,29••].

In the limiting case, in which the contact angle $\theta_\delta = \pi$ on the lyophobic δ domains, the large drop will adapt its contact area to the largest γ domain. Since this drop is large, its $\alpha\beta$ interface has a small mean curvature which implies that all the other γ domains are covered by very thin layers of β phase. This situation can be explicitly calculated for the simple surface domain patterns shown in Fig. 1.

Thus, the wetting layer exhibits two rather different morphologies in the two limits $V_\beta \gg V_\gamma$ and $V_\beta \ll V_\gamma$. This already indicates that it may undergo a morphological transition at an intermediate value $V_\beta = V_c$ as discussed in the next section.

4. Morphological wetting transitions

The three surface domain patterns shown in Fig. 1 lead to morphological wetting transitions which have been studied in some detail as will be described now.

4.1. Circular surface domains

First, consider a pattern consisting of N circular γ domains as shown in Fig. 1a. All domains are taken to have the same diameter L_γ . It is convenient to discuss the limiting case of strongly lyophilic γ domains with contact angle $\theta_\gamma = 0$ and strongly lyophobic δ domains with contact angle $\theta_\delta = \pi$.

For small volumes V_β , the wetting layer consists of N identical droplets which all have the same shape consisting of a small spherical cap. The contact angle θ of this cap is determined by the subvolume V_β/N of each droplet since the usual Young equation is not valid if the contact line is pinned to the $\gamma\delta$ domain boundaries [4••]. As one increases the volume V_β , one attains a certain critical volume at which the wetting layer undergoes a transition to a droplet pattern with one large and $N-1$ small droplets. The large and the small droplets have the same mean curvature M : if one combines one of the small droplets with the large one, one obtains a complete sphere. For larger and larger volumes, the large drop becomes fatter and fatter and the small droplets become thinner and thinner.

4.2. Striped surface domains

Next, consider the striped surface shown in Fig. 1b for which the corresponding wetting morphologies have been determined both theoretically and experimentally [5••]. In the experiments, the β phase was water and the striped hydrophilic domains were created by thermal vapor deposition of MgF_2 onto a hydrophobic silicone rubber or thiolated gold substrate through appropriate masks. The resulting hydrophilic MgF_2 stripes have a width of $30\ \mu\text{m}$ and a contact angle $\theta = \theta_\gamma$ of approximately 5° for water. Both the silicone rubber and the thiolated gold had a contact angle $\theta = \theta_\delta$ of approximately 108° . The projected shape of the channel was studied by optical microscopy, the shape of the contact line by surface plasmon spectroscopy.

When a small amount of water is placed on these stripes, they form homogeneous channels with a uniform cross-section, see Fig. 2a; when the volume V_β exceeds a certain critical value, each of these homogeneous channels undergoes a transition to a new channel state with a single bulge, see Fig. 2b. These different states have also been calculated by minimization of the interfacial free energies of the water channel. The only parameters which enter the calculation are the two contact angles $\theta = \theta_\gamma$ and $\theta = \theta_\delta$ of the hydrophilic and hydrophobic domains, the geometry of the surface domains, and the total volume V_β of water condensed onto these domains. Thus, the theory does not contain any fitting parameter. As shown in Fig. 3, the theoretical shapes agree rather well with the experimental observations.

4.3. Ring-shaped surface domains

Morphological transitions from a channel with uniform cross-section to a channel with a single bulge also occur for ring-shaped surface domains consisting of an annulus with a roughly uniform width as shown

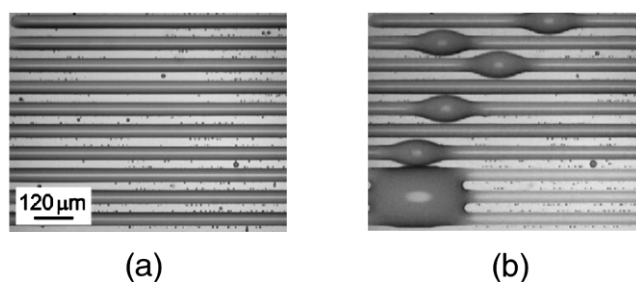


Fig. 2. Channel transition of water channels on a striped surface. (a) If the amount of water per channel is below the critical volume, the channels are thin and homogeneous and their shape is given by cylindrical segments; (b) if the water volume exceeds the critical value, each channel develops a single bulge. The width of both the hydrophilic and the hydrophobic stripes is $30\ \mu\text{m}$.

in Fig. 1c [7•]. In this latter case, the appearance of the bulge breaks the rotational symmetry of the ring channel which implies that the position of the bulge is degenerate. Therefore, angular displacements of this bulge do not cost any (free) energy, and the corresponding interface deformation represents a soft mode which should be observable for domains in the micrometer regime if the β phase is a liquid.

4.4. Bridges across structured slit pores or slabs

Another geometry which can be realized experimentally is slit pores and slabs bounded by structured surfaces [6•,21•]. The first theoretical studies which were performed in the grand-canonical ensemble addressed sinusoidally structured substrates which were investigated by Monte-Carlo simulations [30] and by variational methods [31•]. These systems also exhibit morphological wetting transitions as first pointed out in [32•].

The simplest pattern of surface domains consists of a single pair of opposing lyophilic stripes, see Fig. 4. The two surfaces are separated by L_\perp , the two γ stripes have width L_γ , lie parallel to each other but may be displaced by ΔL as indicated in Fig. 4c. If a certain amount of β phase is placed within such a structured slab, this liquid forms a bridge connecting the two stripes as long as the surface separation L_\perp

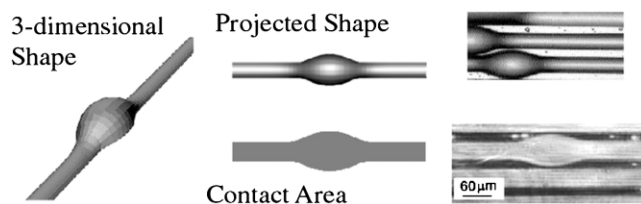


Fig. 3. Channel state with a bulge: comparison of theory (middle) and experiment (right) for the projected shape of the channel and for the shape of the contact line. The drawing on the left shows the full three-dimensional shape as determined theoretically.

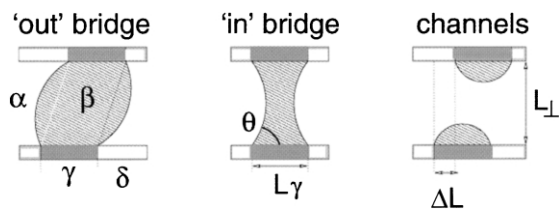


Fig. 4. Different β phase morphologies within a slit pore or slab bounded by two structured surfaces which contain a lyophilic γ stripe: (left) ‘out’ bridge with positive mean curvature; (middle) ‘in’ bridge with negative mean curvature; and (right) Broken bridge or two-channel state. The width of the γ stripes is L_γ , the two surfaces have separation L_\perp , and the two stripes may be displaced laterally by ΔL .

is sufficiently small, see Fig. 4a,b. For larger values of L_\perp , this bridge will break and form two separate channels as in Fig. 4c. This rupture of the bridge provides another example for a morphological wetting transition. In the case of many stripes on the two opposing surfaces of the slab, one has a whole sequence of morphological transitions at which more and more bridges break as one increases the surface separation L_\perp [32•].

If the striped surface domains are relatively long, one may ignore effects arising from their ends. In such a situation, the wetting morphologies are translationally invariant parallel to the stripes and are completely determined by their cross-section as shown in Fig. 4. However, if one takes the finite length of the surface stripes into account, one often finds bridges which are localized in space and, thus, are far from any translationally invariant state; one example is shown in Fig. 5 (A. Valencia, M. Brinkmann and R. Lipowsky, Localized liquid bridges in chemically structured slit pores, in preparation).

4.5. Canonical vs. grand-canonical ensemble

As emphasized, the wetting morphologies discussed above correspond to a canonical ensemble in which the volume of the β phase represents the basic control parameter. In this ensemble, the pressure difference $\Delta P = P_\alpha - P_\beta$ which is conjugate to the volume V_β is related to the mean curvature M via the Laplace equation, $2M\Sigma_{\alpha\beta} = P_\beta - P_\alpha = -\Delta P$, where $\Sigma_{\alpha\beta}$ is the interfacial tension of the $\alpha\beta$ interface. This implies that $\Delta P < 0$ or $P_\beta > P_\alpha$ for $M > 0$ as appropriate for the droplets and channels on a single structured surface. For structured slabs, the ‘out’ and ‘in’ bridges have $M > 0$ and $M < 0$ corresponding to $\Delta P < 0$ and $\Delta P > 0$, respectively.

In the grand-canonical ensemble, however, the pressure difference ΔP is related to the chemical potentials of the particles which can be exchanged with an external reservoir. In this latter case, one must have $\Delta P \geq 0$ for a stable equilibrium state. Thus, apart from the ‘in’ bridges, the morphologies

and morphological transitions discussed above are not accessible within the grand-canonical ensemble.

However, the wetting of structured surfaces can also lead to interfacial phase transitions within the grand-canonical ensemble. One example is provided by a structured surface with a single lyophobic stripe domain [33•,34]. It was found that, depending on the chemical potential and on the stripe width, one can have two different types of adsorption layer for which the layer thickness above the lyophobic stripe is decreased and increased, respectively. Another example is provided by a slab with striped surfaces as studied theoretically in [30,31•,35] within the grand-canonical ensemble. In this case, the presence of the ‘in’ bridges shifts the phase transition lines for capillary condensation. The latter studies were restricted to bridge states which were translationally invariant parallel to the stripes. It remains to be seen how these transitions are affected by localized bridge states as shown in Fig. 5. The grand-canonical ensemble has also been used in order to derive general sum rules for adsorption layers on chemically structured surfaces [36•]; one of these sum rules can be related to the Cassie equation [37].

5. Line tension effects

The morphological wetting transitions, which have been discussed in the previous section, depend only on the free energy contributions arising from the interfaces of the wetting layer. As one studies smaller and smaller systems, the wetting morphologies will also be affected by the free energy or tension of the contact line. The latter quantity, which can be positive or negative [38], was already introduced by Gibbs but its sign and its magnitude is still a matter of intense debate.

5.1. Magnitude of line tension

The numerical values for the contact line tension Λ , which have been deduced experimentally, vary

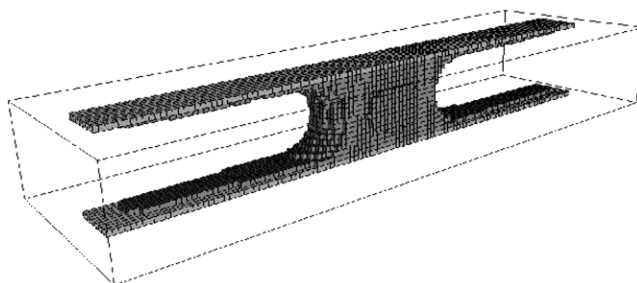


Fig. 5. Localized bridge within a slit pore or slab bounded by two structured surfaces with a lyophilic γ stripe as obtained from canonical lattice gas simulations (A. Valencia, M. Brinkmann and R. Lipowsky, unpublished).

over a wide range as given by $10^{-11} \text{ J/m} \leq |\Lambda| \leq 10^{-6} \text{ J/m}$ [39–42••]. In order to obtain an intuitive understanding of this variation, it is instructive to define an effective width $\ell_{\alpha\beta\sigma}$ of the contact line via $|\Lambda| \equiv (T/\ell_{\text{mol}}^3) \ell_{\alpha\beta\sigma}^2$ where ℓ_{mol} represents a molecular length scale [27•]. The observed range of $|\Lambda|$ values then corresponds to the range $1 \leq \ell_{\alpha\beta\sigma}/\ell_{\text{mol}} \leq 300$ for the effective width of the contact line. These different values for $\ell_{\alpha\beta\sigma}$ presumably reflect different types of small scale heterogeneities which were present on the different substrate surfaces used in the experiments.

The line tension has also been estimated for a lens floating on the vapor–liquid interface of a Lennard–Jones fluid using molecular dynamics simulations [43•]. The line tension value extracted from these simulations is $\Lambda \equiv -10^{-12} \text{ J/m}$ which is somewhat smaller than the theoretical estimates obtained in [38] using local density functionals.

5.2. Surface domains in the nanoregime

It is intuitively clear that the effects of line tension can be ignored for sufficiently large wetting layers. In fact, dimensional analysis implies that the line tension is irrelevant as long as the linear dimensions of the wetting layer are large compared with the characteristic length scale [27•]

$$L_{\beta}^* \equiv |\Lambda|/\Sigma_{\alpha\beta} \quad (1)$$

where $\Sigma_{\alpha\beta}$ denotes the tension of the $\alpha\beta$ interface. The latter tension can be measured by a variety of experimental methods; for water at room temperature, one finds $\Sigma_{\alpha\beta} \cong 72 \text{ mJ/m}^2$. Exceptionally small values for the interfacial tension $\Sigma_{\alpha\beta}$ are observed close to a bulk critical point at which the α and the β phase become identical.

As a typical example, consider an $\alpha\beta$ interface characterized by $\Sigma_{\alpha\beta} \cong 72 \text{ mJ/m}^2$ as appropriate for water and a line tension $|\Lambda|$ of the order of 10^{-9} J/m corresponding to an effective contact line width $\ell_{\alpha\beta\sigma} \cong 3 \text{ nm}$. In this case, the characteristic size L_{β}^* as given by Eq. (1) is $\cong 30 \text{ nm}$, and contributions from the contact line play no role for wetting layers with linear dimensions in the micrometer regime.

However, for surface domains which are comparable to or smaller than $L_{\beta}^* = |\Lambda|/\Sigma_{\alpha\beta}$ the line tension is expected to change the morphologies discussed in Section 4. Thus, a contact line with a positive and negative line tension will try to decrease and increase its length, respectively. For a droplet which can be completely accommodated within a γ or a δ domain, one has the same situation as for a droplet on a homogeneous substrate for which these line tension effects were discussed in [44]. If the droplet is larger and interacts with the $\gamma\delta$ domain boundaries, a con-

tact line with positive line tension may detach from this domain boundary and move across the γ or δ domain in order to shorten its length. Therefore, as one varies the size L_{γ} of the surface domains from $L_{\gamma} \gg L_{\beta}^*$ to $L_{\gamma} \leq L_{\beta}^*$, one expects to find new morphological transitions induced by the line tension. If the wetting structures become sufficiently small, one should also be able to observe thermally-activated transitions between the two states which coexist at a morphological wetting transition.

5.3. Position-dependent line tensions

For a contact line which makes excursions across both types of surface domains, the line tension is expected to be non-uniform and attain the values Λ_{γ} and $\Lambda_{\delta} \neq \Lambda_{\gamma}$ on the γ and δ domains, respectively [27•]. In general, a heterogeneous substrate surface should lead to a position-dependent line tension $\Lambda = \Lambda(x)$ where x denotes the surface coordinate. For a structured surface with arbitrary topography, the contact angle $\theta = \theta(x)$ then satisfies the generalized Young equation [29••]

$$\Sigma_{\alpha\beta} \cos(\theta(x)) = \Sigma_{\alpha\sigma}(x) - \Sigma_{\beta\sigma}(x) - \Lambda(x)C_{\alpha\beta\sigma} - n \cdot \nabla_x \Lambda(x) \quad (2)$$

where the variable $C_{\alpha\beta\sigma}$ is the curvature of the contact line and n is the unit normal vector which is perpendicular both to the contact line and to the normal vector N of the $\alpha\beta$ interface at this line. The symbol ∇_x is the two-dimensional gradient with respect to the coordinate x of the substrate surface.

If the line tension can be ignored, the relation as given by Eq. (2) has the same functional form as the usual Young equation but with x -dependent interfacial tensions $\Sigma_{\alpha\sigma}$ and $\Sigma_{\beta\sigma}$ [4••]. Special cases of the line tension terms have also been derived for planar and homogeneous surfaces [45], for surface heterogeneities which are axially symmetric [46] and for heterogeneities which are translationally invariant with respect to one surface coordinate [47]. The general form of the line tension term as given by Eq. (2) was first obtained in [29••]. One interesting consequence of this general equation is that the contact line exhibits a kink at the $\gamma\delta$ domain boundaries if the line tension $\Lambda = \Lambda(x)$ is piece-wise constant within the γ and the δ domains [27•].

6. Summary and outlook

This review has focussed on morphological wetting transitions, a new concept which was introduced quite recently [4••,5••]. During the last two years, such

transitions have been studied for several surface domain patterns, compare Fig. 1. So far, these studies have focussed on rigid and topographically flat surfaces and on the equilibrium morphologies of the wetting layers.

The wettability contrast between the lyophilic and lyophobic surface domains can also be affected by the topography of these domains. Indeed, the contact angle of a lyophobic surface can be increased by decorating this surface with spikes or other topographical microstructures [48^{••}]. The large contact angles found for some plant leaves also seem to arise from such topographical roughness of the leaf surfaces [49]. Thus, it seems promising to study the effect of such surface topographies on the morphological wetting transitions discussed here. Likewise, one may consider chemically structured surfaces which are not rigid but can deform in response to the wetting layer. One example is a wetting layer on top of a multicomponent membrane which contains intramembrane domains.

Another area of interest is time-dependent relaxation phenomena. For example, consider again the surface domain pattern of N circular domains as shown in Fig. 1a. In the small volume limit, the equilibrium state of the wetting layer consists of N small droplets; in the large volume limit, it consists of $N-1$ small droplets and one large drop. Now, one may initially start with a non-equilibrium state such as a thin layer, which covers many lyophilic and lyophobic surface domains, and follow its time-dependent relaxation into one of the two equilibrium states. Related phenomena are the cooperative evaporation of regular arrays of droplets [50^{••},51[•]] and the dewetting of thin films on chemically heterogeneous substrates [52^{••}].

Finally, the morphological wetting transitions discussed here should be relevant for many applications such as microreactors [5^{••},27[•],53[•]] and microfluidics [15^{••},54^{••},55[•],56[•]].

Please note that the selection of references (marked by • or ••) has been restricted to those published in 1998–2000.

Acknowledgements

I thank Martin Brinkmann, Willi Fenzl, Hartmut Gau, Stephan Herminghaus, Peter Lenz, Peter Swain and Antonio Valencia for fruitful collaborations.

References and recommended reading

- of special interest
- of outstanding interest

- [1] Cahn JW. Critical point wetting. *J Chem Phys* 1977; 66:3667–3672.
 - [2] Ebner C, Saam WF. New phase-transition phenomena in thin argon films. *Phys Rev Lett* 1977;38:1486–1489.
 - [3] Moldover MR, Cahn JW. An Interface phase transition: complete to partial wetting. *Science* 1980;207:1073–1075.
 - [4] Lenz P, Lipowsky R. Morphological transitions of wetting layers on structured surfaces. *Phys Rev Lett* 1998;80:1920–1923.
- Theoretical work which introduced the concept of morphological wetting transitions and determined these transitions for patterns of circular surface domains.
- [5] Gau H, Herminghaus S, Lenz P, Lipowsky R. Liquid morphologies on structured surfaces: from microchannels to microchips. *Science* 1999;283:46–49.
- Comparison of experiment and theory for one specific morphological wetting transition, the channel transition on striped surface domains.
- [6] Silver J, Mi ZH, Takamoto K, Bungay P, Brown J, Powell A.
 - Controlled formation of low-volume liquid pillars between plates with a lattice of wetting patches by use of a second immiscible fluid. *J Coll Interface Sci* 1999;219:81–89.
 A lattice of circular hydrophilic domains is created in the millimeter regime by hydrophobic coating of glass surfaces using screen printing technology.
 - [7] Lenz, P., Fenzl, W., Lipowsky, R. Wetting of ring-shaped domains. *Europhys Lett* 2001; in press.
- Experimental and theoretical study of morphological channel transitions on ring-shaped surface domains.
- [8] López GP, Biebuyck HA, Frisbie CD, Whitesides GM. Imaging of features on surfaces by condensation figures. *Science* 1993;260:647–649.
 - [9] Drelich J, Miller JD, Kumar A, Whitesides GM. Wetting characteristics of liquid drops at heterogeneous surfaces. *Colloids Surf A* 1994;93:1–13.
 - [10] Morhard F, Schumacher J, Lenzenbach A et al. Optical diffraction — a new concept for rapid on-line detection of chemical and biochemical analytes. *Electrochem Soc Proc* 1997;97:1058–1063.
 - [11] Meyer E, Braun HG. Controlled dewetting processes on microstructured surfaces — a new procedure for thin film microstructuring. *Macromol Mater Eng* 2000;276:44–50.
- Thin polystyrene films, which cover a substrate surface with a regular array of lyophobic domains, nucleate holes above these domains and attain a perforated morphology.
- [12] Herminghaus S, Fery A, Reim D. Imaging of droplets of aqueous solutions by tapping-mode scanning force microscopy. *Ultramicroscopy* 1997;69:211–217.
 - [13] Möller G, Harke M, Motschmann H. Controlling microdroplet formation by light. *Langmuir* 1998;14:4955.
- Langmuir–Blodgett monolayers which contain amphiphilic molecules with azobenzene chromophores are patterned by photolithography and lead to regular arrays of water droplets in the micrometer regime.
- [14] Wang R, Parikh AN, Beers JD, Shreve AP, Swanson B.
 - Nonequilibrium pattern formation in Langmuir-phase assisted assembly of alkylsiloxane monolayers. *J Phys Chem B* 1999;103:10149–10157.
 Langmuir–Blodgett monolayers of alkylsiloxane on oxidized silicon substrates are found to exhibit various surface domain shapes.
 - [15] Gleiche M, Chi LF, Fuchs H. Nanoscopic channel lattices with controlled anisotropic wetting. *Nature* 2000;403:173–175. Rapid transfer of DPPC monolayers onto mica surfaces leads to a regular pattern of surface stripes separated by ditches. The stripes and ditches have a width of 800 and 200 nm, respectively.
 - [16] Hayward RC, Saville DA, Aksay IA. Electrophoretic assembly of colloidal crystals with optically tunable micropatterns. *Nature* 2000;404:56–59.

Microsized colloids deposited on an indium tin oxide electrode are found to exhibit regular surface patterns which can be modulated by illumination with ultraviolet light.

- [17] Higgins AM, Jones RAL. Anisotropic spinodal dewetting as a route to self-assembly of patterned surfaces. *Nature* 2000;404:476–478.

Thin films of poly(methyl methacrylate) which are spin-coated onto low-iron glass undergo an anisotropic dewetting process if the glass has been rubbed with lens tissue in one particular direction.

- [18] Burmeister F, Schäfle C, Matthes T, Böhmisch M, Boneberg J, Leiderer P. Colloid monolayers as versatile lithographic masks. *Langmuir* 1997;13:2983–2987.

- [19] Drodofsky U, Stuhler J, Schulze T et al. Hexagonal nanostructures generated by light masks for neutral atoms. *Appl Phys B* 1997;65:755–759.

- [20] Heier J, Kramer EJ, Walheim S, Krausch G. Thin diblock copolymer films on chemically heterogeneous surfaces. *Macromolecules* 1997;30:6610–6614.

- [21] Garcia R, Calleja M, Perez-Murano F. Local oxidation of silicon surfaces by dynamic force microscopy: nanofabrication and water bridge formation. *Appl Phys Lett* 1998;72:2295–2297.

Local oxidation of silicon surfaces by the tip of an atomic force microscope is used in order to create lattices of surface domains with an apparent size of 30 nm.

- [22] Wente HC. A general existence theorem for surfaces of constant mean curvature. *Math Z* 1971;120:277–288.

- [23] Steffen K. On the nonuniqueness of surfaces with constant mean curvature spanning a given contour. *Arch Rat Mech Anal* 1986;94:101–122.

- [24] Struwe M. Plateau's problem and the calculus of variations. Princeton: Princeton University Press, 1988.

- [25] Sullivan JM, Morgan F. Open problems in soap bubble geometry. *Int J Math* 1996;7:833–842.

- [26] Struwe M. Variational methods. Berlin: Springer, 1996.

- [27] Lipowsky R, Lenz P, Swain P. Wetting and dewetting of structured or imprinted surfaces. *Colloids Surf A* 2000;161:3–22.

This review discusses the different microscopic length scales which tend to increase the effective width of the contact line.

- [28] Cassie ABD. Contact angles. *Discuss Faraday Soc* 1948;3:11–16.

- [29] Swain P, Lipowsky R. Contact angles on structured surfaces: a new look at Cassie's and Wenzel's laws. *Langmuir* 1998;14:6772–6780.

Derivation of generalized Young equation for interfacial and line tensions with an arbitrary dependence on the substrate surface coordinate.

- [30] Schön M, Diestler DJ. Liquid vapor coexistence in a chemically heterogeneous slit-nanopore. *Chem Phys Lett* 1997;270:339–344.

- [31] Röcken P, Somoza A, Tarazona P, Findenegg G. Two-stage capillary condensation in pores with structured walls: a non-local density functional study. *J Chem Phys* 1998;108:8689–8697.

Effect on capillary condensation arising from bridge states within the grand-canonical ensemble.

- [32] Swain P, Lipowsky R. Wetting between structured surfaces: liquid bridges and induced forces. *Europhys Lett* 2000;49:203–209.

Morphological wetting transitions related to the rupture of bridges across structured slit pores or slabs.

- [33] Bauer C, Dietrich S, Parry AO. Morphological phase transitions of thin fluid films on chemically structured substrates. *Europhys Lett* 1999;47:474–480.

Interfacial phase transition of an adsorption layer, which covers a structured surface with a single lyophobic stripe, within the grand-canonical ensemble.

- [34] Bauer C, Dietrich S. Phase diagram for morphological transitions of wetting films on chemically structured substrates. *Phys Rev E* 2000;61:1664–1669.

- [35] Schoen M, Bock H. Shear-induced phase transitions in confined lattice gases. *J Phys Condens Matter* 2000;12:A333–A338.

- [36] Henderson JR. Statistical mechanics of patterned inhomogeneous fluid phenomena. *J Phys Condens Matter* 1999;11:629–643.

The grand-canonical potential is used in order to obtain virial theorems and sum rules for fluids which experience a laterally varying force potential arising from a chemically structured substrate surface.

- [37] Henderson JR. Statistical mechanics of Cassie's law. *Molecular Phys* 2000;98:677–681.

- [38] Rowlinson JS, Widom B. Molecular theory of capillarity. Oxford: Clarendon Press, 1982.

- [39] Gaydos J, Neumann AW. Line tension in multiphase equilibrium systems. In: Neumann AW, Spelt JK, editors. Applied surface thermodynamics. New York: Marcel Dekker, 1996:169–238.

- [40] Li D. Drop size dependence of contact angles and line tensions of solid–liquid systems. *Colloids Surf A* 1996;116:1–23.

- [41] Drelich J. The significance and the magnitude of the line tension in three-phase (solid–liquid–fluid) systems. *Colloids Surf A* 1996;116:43–54.

- [42] Pompe T, Fery A, Herminghaus S. Imaging liquid structures on inhomogeneous surfaces by scanning force microscopy. *Langmuir* 1998;14:2585–2588.

The shape profile of water droplets on substrate surfaces is determined by scanning force microscopy. Using a striped surface, the line tension on the hydrophobic part of the surface is estimated to be in the range 10^{-10} – 10^{-9} J/m.

- [43] Bresme F, Quirke N. Computer simulation study of the wetting behavior and line tensions of nanometer size particulates at a liquid–vapor interface. *Phys Rev Lett* 1998;80:3791–3794.

The line tension for a nanoparticle within a liquid–vapor interface is determined by Molecular Dynamics simulations.

- [44] Widom B. Line tension and the shape of a sessile drop. *J Phys Chem* 1995;99:2803–2806.

- [45] Boruvka L, Neumann AW. Generalization of the classical theory of capillarity. *J Chem Phys* 1977;66:5464–5476.

- [46] Rusanov AI. Theory of wetting of elastically deformable bodies. 5. Reduction of the effects of deformation to line tension. *Colloid J USSR (Engl Transl)* 1977;39:618–623.

- [47] Marmur A. Line tension effect on contact angles: axisymmetric and cylindrical systems with rough or heterogeneous solid surfaces. *Colloids Surf A* 1998;136:81–88.

- [48] Bico J, Marzolin C, Quéré D. Pearl drops. *Europhys Lett* 1999;47:220–226.

Hydrophobic surfaces are topographically structured by regular patterns of (i) stripes and ditches, (ii) holes and (iii) spikes which have a size of approximately 1 μm . All of these structures increase the contact angle of water; spikes are most effective and lead to a contact angle close to $\theta = \pi$ corresponding to complete dewetting.

- [49] Barthlott W, Neinhuis C. Purity of the sacred lotus, or escape from contamination in biological surfaces. *Planta* 1997;202:1–8.

- [50] Schäfle C, Bechinger C, Rinn B, David C, Leiderer P.

- Cooperative evaporation in ordered arrays of volatile droplets. *Phys Rev Lett* 1999;83:5302–5305.

A hexagonal lattice of surface domains was created by microcontact printing and then wetted by droplets of diethylene glycol. Slow evaporation of this droplet array leads to a superlattice structure: half of the droplets remain essentially constant in size whereas the others shrink and eventually disappear by evaporation.

- [51] Burghaus R. • Super lattice formation of an array of volatile wetting droplets, *Eur Phys J E* (in press).

- [52] Konnur R, Kargupta K, Sharma A. Instability and morphology of thin liquid films on chemically heterogeneous substrates. *Phys Rev Lett* 2000;84:931–934.

Theoretical work on the rupture of thin films on top of a chemically structured surface. The time evolution of the position-dependent film thickness leads to various two-dimensional wetting morphologies with ‘ripples’ and ‘flowers’.

- [53] DeWitt SH. Microreactors for chemical synthesis. *Curr Opin Chem Biol* 1999;3:350–356.

Review on the fabrication and use of chemical microreactors for

catalytic oxidations, heterocyclic syntheses and photochemical reactions.

- [54] Grunze M. Driven liquids. *Science* 1999;283:41–42.

- Review and comparison of the work on the channel transition in Gao et al. [5] and on microfluidics in Gallardo et al. [55].

- [55] Gallardo BS et al. Electrochemical principles for active control of liquids on submillimeter scales. *Science* 1999;283:57–60.

A regular array of electrodes with a repeat distance in the millimeter range is used in order to modulate the surface tension of an aqueous film which contains redox-active surfactant molecules.

- [56] Schasfoort RBM, Schlautmann S, Hendrikse J, van den Berg

- A. Field-effect flow control for microfabricated fluidic networks. *Science* 1999;286:942–945.

Control of electro-osmotic flow inside microfabricated fluid channels via an additional ‘gate’ electrode attached to the outside of the channel wall.